ELSEVIER

Journal of Nuclear Materials 283–287 (2000) 689–693

journal of nuclear materials

www.elsevier.nl/locate/jnucmat

Phenomenological aspects of fatigue cracking in as-received and hardened F82H modified steel exposed to lithiated water with dissolved hydrogen at 240°C

Marie-Françoise Maday *

Dipartimento Innovazione, Divisione Nuovi Materiali, ENEA-CRE Casaccia, P.B. 2400, I-00100 Rome, Italy

Abstract

The low cycle fatigue (LCF) behaviour of F82H modified steel with three different degrees of hardness produced by specific thermal treatments has been investigated at 240°C under load control, in oxygen-free lithiated solutions containing either no or 2 ppm dissolved hydrogen. In all cases, it was found that the aqueous environments reduced the fatigue life of the material and promoted fracture modes different from those observed in air tests; the fracture modes comprised intergranular and transgranular quasi-cleavage separations as well as microvoid coalescence, which depended on material conditions and water chemistry. All these features were ascribed to a hydrogen-assisted-cracking (HAC) phenomenon, as the basic mechanism for controlling the fatigue behaviour of various F82H heats in lithiated solutions. The observed differences in HAC paths are discussed from the standpoint of material microstructural and substructural parameters. © 2000 Elsevier Science B.V. All rights reserved.

1. Introduction

Environmentally assisted cracking (EAC), leading to premature failure of construction materials, may occur in water-cooled components subjected to simultaneous action of aqueous environment and time-dependent loading. Due to its significance in reactor lifetime and reliability, research has been in progress on the reduced activation martensitic steels (RAMS) for structural applications in fusion systems.

In a previous study [1], low cycle fatigue (LCF) screening tests were conducted on the reference RAMS F82H-modified in as-received condition to evaluate the effects of several water chemistry parameters, namely, pH, conductivity and oxidizing character, on the steel EAC susceptibility. Slightly alkaline (1.5 wppm LiOH: pH $\approx$ 9.8, conductivity $\approx$ 9.3 μS cm^{-1} at room temperature) oxidant-free ($O_2 < 3$ ppb) water appeared as a viable coolant for steel systems from corrosion and corrosion fatigue standpoints and was suggested as a reference environment for future experimental activity. This coolant condition could be practically achieved in fusion devices by employing ^{7}Li-enriched lithium hydroxide as an alkalinizing agent for minimising tritium generation, and by adding hydrogen to suppress radiolytic oxygen and hydrogen peroxide production.

The objective of the present study was to investigate the effect of F82H hardness variation on the EAC behaviour of the steel in the reference water chemistry. This is of interest since the results of the RAMS irradiation test programme indicated that 9Cr–2WV steels suffered severe irradiation hardening at operating temperatures below 400°C, due to the generation of dislocation loops and/or small defect clusters [2]. The influence of dissolved surplus hydrogen in lithiated solutions on the LCF properties of the as-received and hardened F82H alloys is also examined.

2. Experimental details

F82H modified steel with a composition (in wt%) C 0.086, Si 0.1, Mn 0.2, Cr 7.39, W 1.97, S 0.02, P 0.01, Ni

---

* Tel.: +39-6 3048 4391; fax: +39-6 3048 3327.

E-mail address: francoise.maday@enea.casaccia.it (M.-F. Maday).

0022-3115/00/$ - see front matter © 2000 Elsevier Science B.V. All rights reserved.
PII: S 0 0 2 2 - 3 1 1 5 (0 0) 0 0 2 8 0 - 4

0.02, V 0.14, As < 0.005, Sn, Ta < 0.002, Ti, Al, Nb < 0.001, $N_2 : 0.006$, was supplied in the as-received state: namely, austenitized at 1040°C/30 min followed by air cooling (AC) and tempering at 760°C/1 h (designated as A). To simulate pronounced amounts of hardening by irradiation, the following thermal treatments were performed on two batches of the original heat: (a) normalization at 1040°C/30 min + AC; tempering at 625°C/1 h (designated as B) and (b) normalization at 1040°C/30 min + AC (designated as C). Vickers hardness numbers VHN_{10} were 210, 286 and 396 for steels A, B, and C, respectively.

The microstructures and grain/lath morphologies of steels A, B, and C were examined by optical microscopy and scanning electron microscopy (SEM). The fully martensitic matrix contained regions of faulted (steel C) and well defined (steels A and B) laths, inside prior austenite grains of ≈ 90 μm in size. The inclusions were identified by energy-dispersive X-ray microanalysis as: Al, Ti, Ta-rich type-B oxides, and globular Al, -Ti, Ta-rich type-D oxides. No systematic studies were conducted to evaluate the material carbide and substructure as a function of heat treatment, but the hardness trend and the reported information on the microstructures of 9Cr2W(V) steels [3,4] indicate that the martensitic matrix in the normalized state (steel A) will have a high dislocation density but no intra/intergranular carbides. On tempering dislocation recovery and carbide precipitation of the $M(=Cr, W, V)_{23}C_6$ type around grain/lath boundaries and in the matrix, and of the $M(=V, Cr)$ type as fine intragranular dispersion were expected and to a greater extent as the temperature increased. Prediction of coarser carbides in material A was supported by their discernibility as bright particles under back-scattered electron imaging.

Cylindrical tensile specimens machined from each steel were strained to fracture in laboratory air, according to the ASTM E8 standard procedures. The 0.2% offset yield strength $\sigma_{0.2}$, the ultimate tensile strength (UTS), and the ductility indexes – percent total elongation-to-failure ($\%\Delta l$), and percent reduction-in-area (%RA) – obtained at 240°C were:

$$\text{Steel A} : \sigma_{0.2} = 460\ \text{MPa},\ \text{UTS} = 540\ \text{MPa},\ \%\Delta l = 17,\ \%\text{RA} = 79,$$
$$\text{Steel B} : \sigma_{0.2} = 698\ \text{MPa},\ \text{UTS} = 762\ \text{MPa},\ \%\Delta l = 13,\ \%\text{RA} = 77,$$
$$\text{Steel C} : \sigma_{0.2} = 988\ \text{MPa},\ \text{UTS} = 1279\ \text{MPa},\ \%\Delta l = 9.7,\ \%\text{RA} = 41.$$

The recirculating autoclave system and experimental equipment used for the LCF tests have been described elsewhere [5]. The testing environments consisted of (a) 240°C flowing air and (b) 240°C/45 atm flowing (9 l/h) lithiated solution (1.5 wppm LiOH). A dissolved oxygen content of <3 wppb was maintained by automatic purging of argon during the tests and the dissolved hydrogen level could be controlled to 2 wppm by pressurized hydrogen gas. Hourglass specimens 7.5 mm in diameter were tested by LCF to rupture. Tests were conducted under load control in accordance with the ASTM Standard E606 by using a fully reversed triangular load waveform at a rate of 2.2 kN/s (50 MPa/s). The load amplitudes suitable for the LCF regime, were selected to ensure sufficient time for environmental effects to occur, within an acceptable test duration. The corrosion potentials of the steels were continuously recorded against an Ag/AgCl reference electrode. Fracture surfaces and profiles were observed by SEM and optical microscopy after cleaning with hydrochloric acid.

3. Experimental results

The average numbers of cycles to specimen rupture from duplicate tests performed on steels A, B, C at 240°C in air and in the lithiated solutions are shown in Figs. 1 and 2. The degree of scatter was less than 5%. The data indicated that LiOH-dosed water caused a reduction in fatigue life of all the three samples when compared with the results obtained in air. The fracture surfaces typically contained a semi-elliptic subcritical crack, which started from the specimen periphery and was followed by the overload cracking region which terminated in a shear lip. Similar fatigue lives and macroscopic features were obtained after fracturing specimens B and C in lithiated water with 2 ppm dissolved hydrogen, while specimen A suffered an additional fatigue lifetime loss ($\approx 30\%$) and exhibited an almost uniform necking which is not observed in the hydrogen-free solution or in the air. The presence of a central fibrous zone on the fracture surface suggested that crack formation and stable growth occurred internally, before merging with the surface.

A detailed fractographic analysis was performed on specimens A, B, C tested under the lowest stress amplitude of their respective intervals where the most environmental susceptibility was observed. The overload fractures always exhibited the classical dimple patterns. In stable crack growth regions, the crack that developed in air and in aqueous environments differed in their first half portion starting from the specimen edges, but became similar during the subsequent transition regime. The reference morphologies of the cracks formed in air are shown on fractograph Fig. 1(a) for steel A and on fractographs in Fig. 2(a) and (c) for steels B and C, respectively. Fatigue cracking was of the ductile type in steels A and B, and propagated on several parallel plateaus with pronounced (Fig. 1(a)) or poorly-defined (Fig. 2(a)) striations, while brittle cleavage occurred in steel C (Fig. 2(c)).

In lithiated water, these features changed in both steels A and B to another type of transgranular unstriated separation, scarcely crystallographic but showing evidence of plasticity and secondary cracking, features

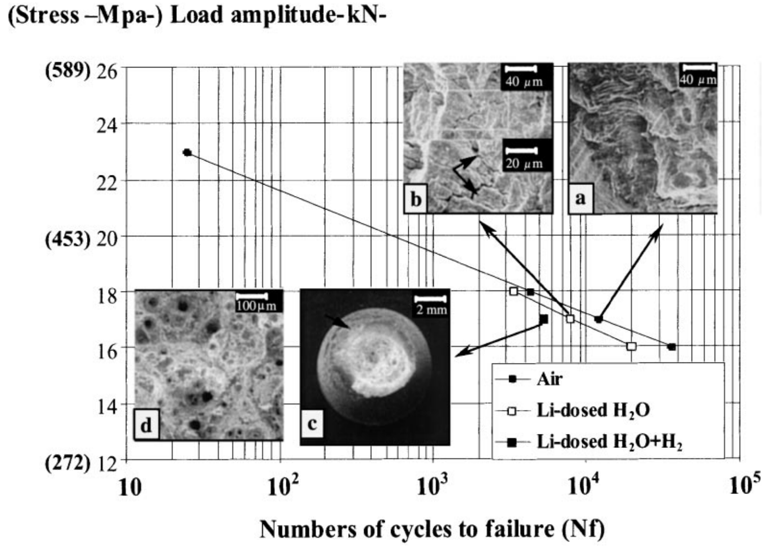

Fig. 1. LCF results of F82H steel A after testing in air and in lithiated-water environments with and without dissolved hydrogen.

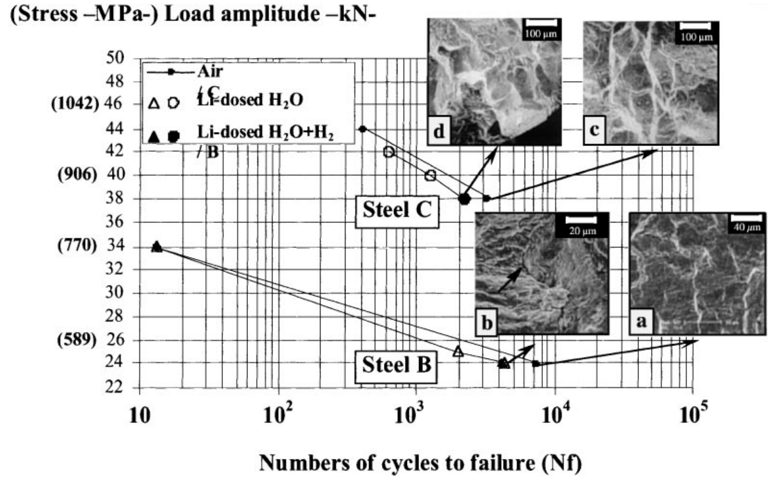

Fig. 2. LCF results of F82H steels B and C after testing at 240°C in air and in lithiated-water environments with and without dissolved hydrogen.

associated with tempered martensite microstructure (arrows in Figs. 1(b) and 2(b)), and to a mixed intergranular/cleavage cracking in steel C (Fig. 2(d)).

The same morphologies persisted in specimens B and C after testing in hydrogen-added lithiated solutions, while specimen A failed almost completely by microvoid coalescence (MVC) (Fig. 1(d)) with a fracture appearance resembling the cup and cone mode. Incipient cracks were found around the periphery and multiple crack nucleation along the necked gage length was associated with coarse persistent slip bands (arrow in Fig. 1(c)).

The open circuit potential of F82H depended on water chemistry but was unaffected by the heat treatment. Steady values of -0.78 ± 0.02 V and -0.7 ± 0.02 V (against the standard hydrogen electrode, SHE) in lithiated water with and without dissolved hydrogen, respectively, were quickly reached upon heating and were maintained during the entire test.

4. Discussion

The fracture features, produced by pure mechanical fatigue in air, on the stable cracks of steels A, B and C showed an increasing brittle character as hardness increased and reflected differences in plastic accomodation during crack growth. This occurs in steels A and B by dislocation glide on more (steel A) or less (steel B) numerous active shear planes (strain-induced), starting from the specimen surface at emergent slip steps by atomic bond rupture along cleavage planes (stress-induced) crossing each grain with initiation probably located at subsurface dislocation pile-ups.

Different patterns observed in the first portion of cracking in water, and the occurrence of MVC in one case, indicated that an environment-related effect dominated over mechanical fatigue, and it could be induced either directly (anodic EAC) or indirectly (cathodic EAC) by the corrosion process. Discrimination between these alternatives has been helped by comparing our fracture results with well-identified reference fractographs [6–9]: the particular form of 'quasi-cleavage' in steels A and B (denoted also QC_{HE} [6] or chisel [7]), the intergranular cracking of the stronger steel C, and the observed transition from QC_{HE} fracture to MVC in steel A, were different variants of martensitic steel failure by HAC. Such a model appeared probable, since HAC in aqueous environments results essentially from cathodic hydrogen produced in its atomic form (H), and, just as in the present case, may occur in a susceptible matrix when H discharge via water reduction results for balancing metal corrosion. According to the current description, atomic H is supplied to any potential fracture process region inside the host metal through the sequence of surface reaction, absorption and diffusion, where it is equilibrated among the various matrix elements (lattice sites and traps). For a given material/stress combination, the propensity to a particular cracking mode depends on the temperature and H discharge, and reflects the occurrence in the process zone of a kinetically favoured [10] detrimental interaction between material and hydrogen.

By considering the steel/environment combinations of this study, it is anticipated that: (i) at the testing temperature 240°C, H affected mainly the martensitic matrix by reducing the cohesive strength of interfaces and interatomic bonds of specific crystallographic planes, and by promoting flow localization on particular slip systems [11]; (ii) the hydrogen traps which remained active at 240°C and could act as crack nuclei were: grain and lath boundaries, oxide inclusions and intergranular, inter/intralath carbides in the tempered microstructures, and clean grain/lath boundaries and inclusions in the normalized steel, while dislocations were probably not effective; and (iii) the amount of cathodic hydrogen supplied in the discharge reaction depended on the water chemistry but was irrespective of material heat treatments, as suggested from the elctrochemical results.

In lithiated water and under cyclic loadings, where a critical crack embryo nucleated (either aided or not by H) in all the steels, cathodic H, discharged at the bare tip to sustain steel corrosion and at the passive specimen surface to sustain steel oxidation, was driven in the maximum triaxial stress field under the induced chemical potential gradient. In this process zone, sufficient H was gained for reducing the cohesive strength of specific interfaces. The most detrimental effect occurred (i) at lath/lath packets boundaries in steels A and B causing their opening (stress-induced), while cracking propagated on glide planes through H-enhanced flow localization (strain-induced); (ii) under the additional stress from dislocation pile-up, at 'clean' grain boundaries, which served as crack nuclei and paths (both stress-induced).

H is currently expected [12] to promote MVC by lowering the bond strength of particle/matrix interfaces, and by enhancing void nucleation and expansion through flow localization. Experimentally [13], MVC is favoured when sufficient H is distributed over a plastic zone large enough to involve many inclusions acting as potential void nuclei (high H-supply case), and competes with QC_{HE}, conversely associated with the concentration of hydrogen and plasticity in a region too small to include a sufficient number of particles (low H-supply case). The transition from QC_{HE} to MVC in steel A, and the multiple crack initiation (unfavourable for triaxial stress build-up) due to enhanced shear instabilities at the specimen surface (often attributed to H) agreed with a high H-supply condition in hydrogen-dosed lithiated water. The phenomenon did not occur in steels B and C which were exposed to the same environment, but had microstructural differences in terms of hardness and carbide distribution leading probably to: (i) the delay/inhibition of H-induced enhancement of shear instabilities due to dislocation interaction, (ii) the lack of effective sites for H-induced void nucleation due to the absence of carbides in steel C and weak H-trapping character of the finer coherent carbides of steel B. The argument as to why lithiated water with dissolved molecular hydrogen apparently provided more cathodic H to steels, may have an electrochemical foundation and must be clarified.

5. Conclusions

- F82H steels with different degrees of hardness and microstructures were susceptible to EAC in 240°C lithiated-water environments, which reduced fatigue life and exhibited different failure modes compared to those observed in air.
- A comparison of the fractographic results with those of well-identified mechanisms suggested that different EAC fracture patterns were variations of HAC phenomenon, resulting from atomic hydrogen discharged to sustain steel corrosion.
- Grain/lath boundaries and carbide/matrix interfaces weakened by atomic H were all potential sites for premature microcrack formation in the process zone.

Subsequent crack growth occurred by breaking the weakest interface or interatomic bond (stress-induced) in the harder steel without plasticity, and by dislocation glide on preferential planes (strain-induced) as hardness decreased.

- The complete MVC failure of the 'softer' steel fatigue-tested in lithiated water with dissolved hydrogen, suggests a more efficient H supply to the steel in such environment, but needs further assessment.

References

[1] M.F. Maday, Fus. Technol. 2 (1998) 1207.
[2] F. Abe, T. Noda, H. Araki, M. Narui, H. Kayano, J. Nucl. Mater. 166 (1989) 265.
[3] R.L. Klueh, P.J. Maziasz, Metall. Trans. A 20 (1989) 373.
[4] R.L. Klueh, D.J. Alexander, E.A. Kenik, J. Nucl. Mater. 227 (1995) 11.
[5] M.F. Maday, J. Nucl. Mater. 233–237 (1996) 1397.
[6] Y. Kikuta, T. Araki, in: Strauss/Cullen (Eds.), Fractography in Failure Analysis, ASTM STP 645, American Society for Testing and Materials, Philadelphia, PA, 1978, p. 107.
[7] C.A. Hippsley, N.P. Hawaorth, Mater. Sci. Technol. 4 (1988) 791.
[8] W.W. Gerberich, T. Livne, X.F. Chen, M. Kaczorowski, Metall. Trans. A 19 (1988) 1319.
[9] T.P. Perng, C.J. Altstetter, Metall. Trans. A 18 (1987) 123.
[10] M. Gao, M. Lu, R.P. Wei, Metall. Trans. A 15 (1984) 735.
[11] H.K. Birnbaum, NACE 10 (1990) 21.
[12] N.P. Haworth, C.A. Hippsley, UKAEA Report AERE R-11473, Harwell Laboratory, 1985.
[13] T.P. Perng, C.J. Altstetter, Metall. Trans. A 18 (1987) 735.